# High-Efficiency Adsorption and Sustainable Desorption of Anionic Dyes Using a Novel AC–$Fe_2O_3$/ZnO Nanocomposite

**Ayat S. Al-Maliki[1] , Dunya A. Al-Abbawy [1,*] and Zuhair A. Abdulnabi [2]**

[1] Department of Ecology, College of Science, University of Basrah, Basrah, Iraq.
[2] Department of Marine Chemistry, Marine Science Center, University of Basrah, Basrah, Iraq.

[*]**Corresponding author E-mail:** dunya.hussain@uobasrah.edu.iq

https://doi.org/10.29072/basjs.20260121

**ARTICLE INFO**

*Received: 16 January 2026*

*Accepted: 12 March 2026*

*Published: 30 April 2026*



***Keywords:***

*Activated carbon, Eosin Blue, Fuschin Acid, zinc oxide, organic pollutants, Recovery study*

**ABSTRACT**

This study proposes the preparation of a novel adsorbent material, AC-ZnO-$Fe_2O_3$, synthesized using activated carbon derived from plastic waste and metal oxides produced via co-precipitation methods. The structural and physicochemical characteristics of the prepared adsorbent were examined using FTIR, XRD, BET, and EDX analyses. Particle size estimation performed by SEM revealed values of 63.29 nm for activated carbon (AC), 91.69 nm for $Fe_2O_3$, 68.79 nm for ZnO, and 72.11 nm for the composite (AC-ZnO-$Fe_2O_3$). Zeta potential measurement recorded a negative surface charge of it-42.2 mV. The batch adsorption technique was employed to evaluate the removal efficiency of two anionic dyes, Eosin Blue (EB) and Fuchsin Acid (FA), under varying operational conditions, including equilibrium time, temperature, pH, and agitation speed. Under optimal conditions, the removal efficiencies reached 77.17% and 88.21% for EB and FA, respectively. Adsorption isotherm analyses demonstrated that the Freundlich model provided the best results. In addition, thermodynamic parameters were calculated, and a negative $\Delta G^{o}$ value was obtained, indicating a spontaneous adsorption process and confirming the endothermic nature of the reaction. Finally, Desorption experiments were conducted to achieve high recovery efficiencies of 98.46% For EB and 75.81% For FA, using water as the solvent.

## 1. Introduction

Environmental pollution has become one of the most pressing global challenges, threatening both ecosystems and human health [1]. In recent decades, rapid technological development and industrial expansion have intensified the release of contaminants into natural systems, thereby exacerbating environmental pollution [2-3]. Among the various forms of pollution, water contamination remains a critical issue because of its direct impact on life, agriculture, and industry [4]. Water pollution is defined as any alteration in the physical, chemical, or biological characteristics of water that renders it unsuitable for its intended use [5]. Pollutants present in aquatic systems can be broadly categorized into as inorganic pollutants, such as heavy metals, and organic pollutants, including dyes, hydrocarbons, and pesticides. Both pose severe environmental and health risks [6]. Synthetic dyes are among the most persistent and hazardous organic pollutants and are widely used in the textile, plastic, paper, cosmetics, rubber, and leather industries [7].

The inherent physicochemical stability of these compounds, coupled with their resistance to biodegradation, renders them particularly persistent in aquatic environments and difficult to remove using conventional treatment processes [8]. Their discharge into water bodies significantly reduces light penetration, thereby limiting photosynthetic activity and impairing primary productivity. This disruption subsequently contributes to a decline in dissolved oxygen concentrations, adversely affecting aquatic ecosystems. In addition, to these ecological impacts several studies have highlighted their potential to induced mutagenic and carcinogenic effects, posing serious risks to environmental and human health [9-11]. Among the wide spectrum of synthetic dyes, Eosin Blue (EB) and Fuchsin Acid (FA) have attracted particular concern due to their persistence and environmental impact. Eosin Blue is an anionic xanthene dye characterized by high aqueous solubility and widespread application in textile dyeing, ink production, and biological staining processes [12-13]. In contrast, Fuchsin Acid belongs to triphenylmethane class of anipnic dyes and is distinguished by a highly conjugated chromophoric structure that imparts strong color stability and resistance to degradation, thereby enhancing its environmental persistence [14-15]. Therefore, the development of cost-effective, efficient, and eco-friendly remediation technologies is essential for the sustainable treatment of dye-contaminated wastewater [16]. Among the several existing methods, adsorption stands out because of its high efficiency, operational simplicity, low cost, and environmental compatibility [17-19]. Activated carbon (AC) remains the most widely used adsorbent, offering a large surface area, high porosity, and chemical stability [20]. It is easily regenerated and produced from

sustainable materials such as fruit peels, coconut shells, and single-use plastic waste [21-22]. In recent years, nanomaterials have gained significant attention owing to their unique physicochemical, optical, and magnetic properties, primarily resulting from their nanoscale dimensions and high surface-to-volume ratio [23-24]. Metal oxidizes nanoparticles such as Ag, ZnO, $TiO_2$, and $Fe_2O_3$ have demonstrated remarkable potential in water purification applications, while mixed metals oxides (e.g., Fe-Mn, Fe-Ti, Fe-Cr) exhibit synergistic effects that further enhance adsorption efficiency and stability [25-26]. This study aims to investigate the effectiveness of integrating activated carbon with metal oxide nanoparticles, offering a sustainable and highly effective approach for removing persistent dyes such as Eosin blue and Fuchsin Acid. This is achieved by combining the high surface area and adsorption capacity of activated carbon with the catalytic and reactive characteristics of nanostructured oxidized to achieve superior performance through synergistic interaction.

## 2. Materials and Methods

### 2.1. Chemicals

All chemicals used in this study were of analytical grade. Ammonium hydroxide (25%), NaOH and KOH were Obtained from Merck. Hydrochloric acid (37%) and nitric acid (65%) were supplied by GCC, and concentrated sulfuric acid (95%) was purchased from J.T. Baker. Ferric citrate[$C_6H_5O_7Fe.5H_2O$] and the dyes EB and FA were provided by BDH. Zinc acetate dihydrate [Zn $(CH_3COO)_2$ $.2H_2O$] was obtained from Riedel-De Haen Agseelze Hannover, and ethanol (96%) from Fisher chemical.

### 2.2. Instrumentation

The functional groups on the surface of the prepared adsorbent were identified using FTIR in the range of 400–4000 $cm^{-1}$ with a Shimadzu FTIR -8400s Spectrophotometer. The maximum adsorption wavelength was determined using a Shimadzu UV-Vis 1800 spectrophotometer. The surface morphology and elemental composition were examined via SEM and EDX using a Vega A3 microscope at 20kV. The crystalline phase and crystallite size were analyzed by XRD using a Philips PW1370 diffractometer with Cu Kα radiation (λ= 1.54$A^{o}$). Additionally, EDX analysis was performed using a Zeiss microscope to determine the elemental composition of the prepared adsorbent.

### 2.3. Synthesis of AC-ZnO-$Fe_2O_3$ Nanocomposite

Activated carbon (AC) was prepared from plastic waste collected from different source (drinking water bottles made of polyethylene terephthalate). The waste was washed with deionized water, dried at 65 $^{o}$C, crushed, and sieved (2 mm). A 25 g portion of the material was mixed with 25 mL of concentrated sulfuric acid ($H_2SO_4$) and stirred magnetically at 90 $^{o}$C for 2h. The resulting black carbonaceous material was washed several times with deionized water and dried at 80 $^{o}$C for 4h, followed by carbonization at 300 $^{o}$C for 3h [22]. The sample was filtered and dried again at 80 $^{o}$C for 5h. It was then oxidized with 32.5% nitric acid ($HNO_3$) under continuous stirring at 60 $^{o}$C for 5h, washed with deionized water until neutral pH, and dried at 80 $^{o}$C the preparation method was depended [27].

Nanostructured metal oxidizes zinc oxide (ZnO), and ferric oxide ($Fe_2O_3$) were synthesized via the co-precipitation method . For ZnO nanoparticles were prepared by dissolving 2.19809 g of zinc acetate dihydrate in 300mL of distilled water under magnetic stirring. A KOH solution (1.2155 g in 50 mL distilled water) was added gradually until a white precipitate formed. The precipitate was then calcined at 400 $^{o}$C for 180 min to obtain ZnO nanoparticles [29-30]. Similarly, $Fe_2O_3$ nanoparticles, dissolved (1 g) of ferric citrate was dissolved in 100 mL of distilled water to form an orange solution. The pH was adjusted to neutrality using NaOH (1%), followed by the addition of ethanol to induce precipitation. The precipitate was separated by decantation, washed several times with ethanol, dried at 200 $^{o}$C, and calcined at 300 $^{o}$C [28].

Finally, the synthesized ZnO and $Fe_2O_3$ nanoparticles were supported onto the activated carbon surface to obtain the AC-ZnO-$Fe_2O_3$ nanocomposite. ZnO and $Fe_2O_3$ nanoparticles (0.04 g each) were dispersed in 40mL of deionized water, followed by the addition of 0.2 g of activated carbon. The mixture was sonicated for 60 min to ensure uniform dispersion and then subjected to hydrothermal treatment at 180 $^{\circ}$C for 4h. The resulting composite was separated, washed, and dried at 80 $^{o}$C for 3hours to obtain the final AC-ZnO-$Fe_2O_3$ nanocomposite [30].

### 2.4. Preparation standard solutions of Eosin Blue and Fuchsin Acid dyes

A standard stock solution with a concentration of 1000 mg/L was prepared, and various dye concentrations were subsequently prepared. The maximum wavelength of Eosin Blue (EB) and Fuchsin Acid (FA) was determined using 10 mg/L, and then measured using a UV-Vis spectrophotometer within a wavelength range of 200–800 nm. The results indicated that the maximum wavelengths were 518.5 nm and 546.5 nm for EB and FA, respectively.

### 2.5. Experiments of Adsorption

The adsorption process refers to the retention of ions, atoms, or molecules from liquids, gases, or dissolved solids onto the surface of a solid material. This phenomenon provides valuable insights into the nature of the adsorbed molecules, characteristics of the adsorbent surface, and interaction mechanisms between them [31]. In this study, adsorption experiments were conducted to remove anionic dyes from aqueous solutions and determine the optimal conditions for adsorption, including equilibrium time, pH, temperature, and mixing speed. These experiments were designed to evaluate the adsorption efficiency of the prepared adsorbent under controlled laboratory conditions. Each experiment was performed using 10mL of dyes solution with initial concentrations of 100 and 200 mg/L for Eosin blue and Fuchsin Acid, respectively.

A0.01g portion of the previously prepared adsorbent was used, and the solutions were agitated at a speed of 150 rpm under neutral pH and room temperature to determine the equilibrium time for each dye .The removal percentage and adsorption capacity were calculated using the following equations [32]:

$$\% \text{ AD} = [(\text{Co-Ce})/\text{Co}] \times 100$$

$$\text{Qe (mg/g)} = [\ \text{V}\times(\text{Co-Ce})]/\ \text{W}$$

:Where

AD% is the adsorption ratio

C0 is the initial dye concentration, (mg/L)

Ce is the equilibrium dye concentration (mg/L)

Qe is the adsorption capacity (mg/g) V is the volume of the dye solution (L)

W is the mass of the adsorbent (g)

The adsorption isotherm experiments were conducted under different conditions from those in the optimization study. The initial dye concentrations and solution volumes were increased to obtain sufficient mass of adsorbate for the adsorbent dose, and thus to accurately estimate the equilibrium parameters. This resulted in a total amount of dyes greater than the adsorption capacity of the adsorbents, and thus the Langmuir Qmax values fit the mass balance.

All experiments were performed in triplicate, and the reported values represent the mean ± standard deviation (SD).

### 2.6. Adsorption Isotherm

Adsorption isotherms describe the relationship between the amount of adsorbate retained on the surface of the adsorbent and its concentration in solution at a constant temperature (equilibrium state). Studying adsorption isotherms helps to understand the phenomenon associated with the adsorption process, the interaction between the adsorbent surface and dye molecules, and provides valuable insights into the thermodynamic behavior of adsorption systems. In the present study, two isotherm models were employed to describe the adsorption behavior: The Langmuir and Freundlich isotherms [33]. The Langmuir isotherm assumes that adsorption occurs on a homogeneous surface in a monolayer manner and that the process can be either physical or chemical, depending on the type of bonding between the adsorbate molecules and the adsorbent surface. The Langmuir model is expressed by the following equation [17]:

$$C_e/Q_e = (1/ (Q_{max} \times K_L)) + (C_e/Q_{max})$$

Where:

$Q_{max}$(mg/g) represents the maximum adsorption capacity for dye molecules at constant temperature

$K_L$ (L/mg) is the Langmuir constant related to the affinity of binding sites

on the other hand, The Freundlich isotherm, is generally applied to describe physical adsorption on heterogeneous surfaces, where multilayer adsorption occurs [34]. It is represented by the following equation:

$\text{Log } Q_e = \text{Log } Kf + (\text{Log } C_e/n)$

Where:

Kf is the Freundlich constant indicating adsorption capacity

The value of the heterogeneity factor (n) indicates the favorability of the adsorption process

When n>1: the adsorption process is favorable and efficient (strong adsorption)
When 0<n<1: the adsorption process is weak or unfavorable
When n=0, the adsorption process is irreversible or does not occur.

### 2.7. Recovery

This study was conducted to recover the molecules of Eosin Blue and Fuchsin Acid dyes and returned them to the solution after completing the adsorption process under the selected optimum condition. The adsorbent material (0.01 g) and dye solution (10 mL) were taken, and

the mixture was separated using a centrifuge at 4500 rpm for 10 min. Water was used as a recovery solvent to break the bond formed between the dye molecules and the adsorbent surface molecules, and then it was liberated to solution once again and measured at the selected wavelength. The recovery percentage of the dyes was calculated using the following equation [35]:

$$\%R_e = [C_L/ (C_0-C_e)] \times 100$$

Where the Re is represented recovery ratio and CL is liberated concentration in solution by unit mg/L

## 3. Results and discussion

### 3.1 FTIR characterization

The FTIR spectra of activated carbon (AC) and oxidized activated carbon (OAC) were examined to identify surface functional groups and verify the effectiveness of the oxidation treatment. The spectra displayed characteristic absorption bands at 3063.7 $cm^{-1}$, corresponding to aromatic C-H stretching vibrations, and at 2970.6-2814.6 $cm^{-1}$, attributed to aliphatic C-H stretching. A strong band observed at 1677 $cm^{-1}$ is associated with C=C and/or C=O stretching vibrations, while the bands in the range of 1572.4 -1418.7 $cm^{-1}$ indicate the presence of benzene ring structures. Additional bands at 1282.7 and 1110.2 -1014.7 $cm^{-1}$ are assigned to C-O and C-O-C functional groups, respectively. Following nitric acid oxidation, the OAC spectrum exhibited a broad band centered around 3400$cm^{-1}$, corresponding to -OH groups. The appearance and increased intensity of this band confirm the introduction of oxygen-containing functional groups, indicating successful surface oxidation and enhanced hydrophilicity of the modified carbon [36].

The FTIR spectrum of the oxide synthesized via the co-precipitation method exhibited strong absorption bands at 498.14 and 624.7$cm^{-1}$, which are attributed to the Zn-O stretching vibrations. Additionally, prominent bands were observed at 532.1 and 436.9 $cm^{-1}$, along with abroad band centered at 1050.2 $cm^{-1}$, corresponding to the Fe-O and Fe-OOH vibrations. These results confirm the successful formation of zinc oxide and iron oxide phases **[37]**. Furthermore, the FTIR spectrum of the synthesized AC-$Fe_2O_3$ and ZnO showed vibrations at 460.4 -646.9 $cm^{-1}$, confirming the successful formation and loading of metal oxides onto the activated carbon surface. The decrease in the intensity of the carbon-related bands (–OH, C=O, C-O, and C-O-C) suggests a strong interaction between the oxide and the functional groups of the carbon matrix [21] as shown in Figure1.

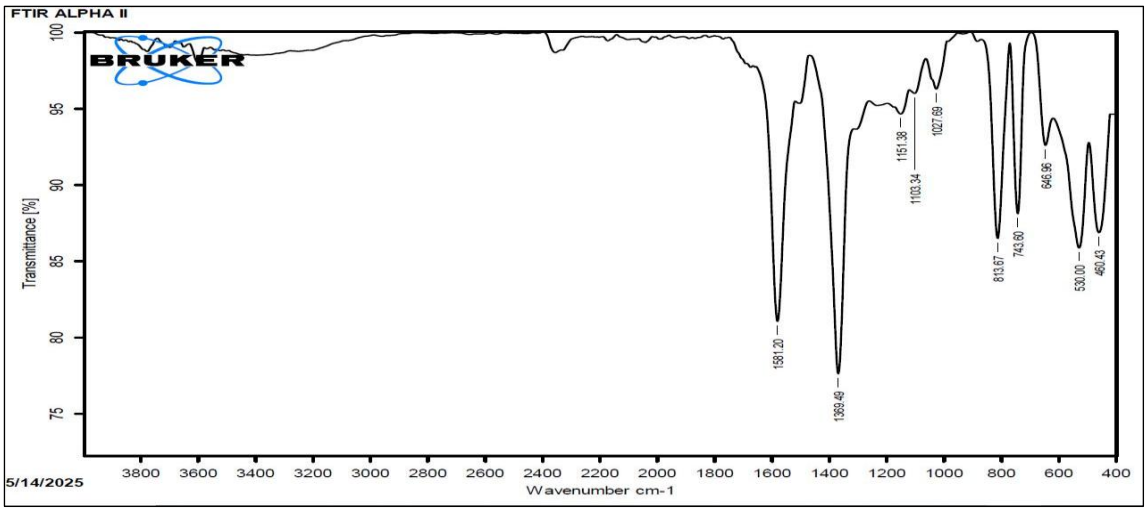


**Figure 1.** The FTIR result of prepared surface AC-ZnO and $Fe_2O_3$ composite

### 3.2 BET analysis

The porous structure of the prepared composite plays a crucial role in the adsorption process, as it facilitates the diffusion and interaction of pollutant molecules through the pores, in addition to the contribution of the surface functional groups.

The Brunauer-Emmett-Teller (BET) method was employed to determine the specific surface area and pore characteristics of the synthesized carbon-based composite loaded with zinc and ferric oxidase. The obtained results revealed that the prepared surface exhibited a specific surface area of 4.6932 $m^2/g$, indicating the presence of a porous texture that enhances the adsorption capability of the composite materials (Table1).

The low BET surface area of the composite is attributed to the following factors. The activated carbon was prepared from plastic waste and carbonized at a very low temperature (300 $^{\circ}C$), which could not contribute to the formation of a well-defined microporous structure. Second, the loading of $Fe_2O_3$ and ZnO nanoparticles into the carbon matrix partially blocked the pore entrance, thereby decreasing the surface area. Similar results of BET surface area reduction after incorporating metal oxides into the carbon matrix have been reported in previous studies. The low surface area of the composite did not affect the high adsorption performance, which shows that adsorption is not only dependent on the surface area but also on the surface functional groups, electrostatic attractions, and chemical affinity of interaction between the dye and the active sites [22, 38].

The BET surface area of the composite was relatively low (4.69 $m^2/g$), but the adsorption capacity was very high. This implies that the physical surface area alone was not responsible for adsorption performance. In addition to the introduction of oxygen-containing functional groups (–OH and –COOH) by nitric acid oxidation, $Fe_2O_3$ and ZnO nanoparticles added additional active sites. These surface functionalities can facilitate electrostatic attraction,

surface complexation, and possibly chemisorption of the dye molecules. The BET surface area is a nitrogen-accessible surface area of the dry material and may not accurately represent the available adsorption sites for large organic molecules in an aqueous environment. Similar reports of high adsorption capacity with a low BET surface area also exist for functionalized/metal-loaded carbon-based composites.

**Table 1.** The BET result of AC-ZnO-$Fe_2O_3$

| Adsorption surface | Surface Area $m^2/g$ | Pore volume $cm^3/g$ | Pore diameter nm | Pore type |
|---|---|---|---|---|
| AC-ZnO- $Fe_2O_3$ | 4.6932 | 0.0308 | 2.4 | Mesopores |

### 3.3 X-ray powder diffraction

X-ray diffraction (XRD) was employed to determine the crystalline phase, crystal size, and degree of crystallinity of the prepared materials [39]. Distinct diffraction peaks indicate the material type and its crystallinity. For the activated carbon synthesized from plastic waste, characteristic peaks appeared at 2θ= 21.3°, 23.05°, 24.86°, 25.59°, 26.8°, 32.08°, and 38.19°, corresponding to the standard JCPDS card no. 41-1487. The prominent peak at 2θ = 25.59° confirms the successful synthesis of activated carbon (Figure 2) [19].

The crystallite size (D) was estimated using the Debye-Scherrer equation [40]:

$D=K\lambda/\beta \cos \theta$

Where K=0.9, ƛ= 1.54A (Cu kα), β is the full width at half maximum of the peak, and θ is the Bragg angle.

For zinc oxide (ZnO), the XRD pattern exhibited multiple peaks at 2θ = 23.03°, 25.40°, 34.77°,36.56 °,38.35 °,47.9 °,56.86 °, 63.38 °, 66.9 °,69.72 °, and 77.8°, which match the standard JCPDS card no. 36-1451 [41].

Similarly, the XRD pattern of ferric oxidize ($Fe_2O_3$) showed peaks at 2θ = 24.40°, 25.42° ,32.20°,33.54 °, 36.10°, 38.27°, 41.29°, 49.98° , 54.59° , 58.09° , 62.96°, 64.45°,consistent with JCPDS card no. 86-0550 confirming the successful co-precipitation synthesis of hematite

The XRD pattern of the AC-ZnO-$Fe_2O_3$ composite displayed characteristic peaks of AC at 2θ =12.18°, 17.07°, 25.59° peaks corresponding to $Fe_2O_3$ at 2θ = 24.37°, 33.34°, 54.28° ,58.88°. And peaks for ZnO at 2θ = 35.83° ,45.6° ,49.62° ,62.78° ,64.36° ,72.18°, confirming the successful hydrothermal loading of both metals oxidize onto the activated carbon surface [42].

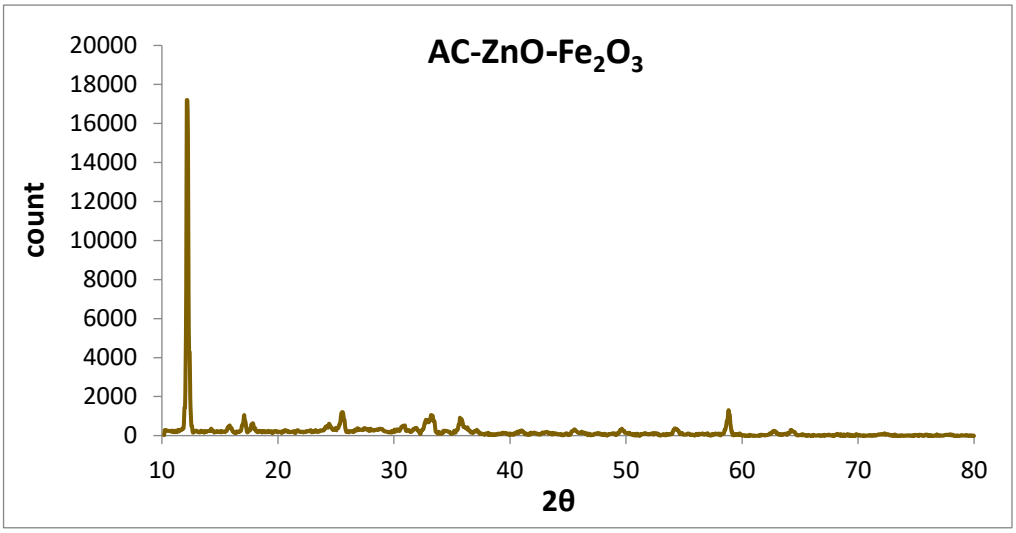


**Figure 2.** The XRD patterns of AC-ZnO -$Fe_2O_3$ composite

### 3.4 Scanning Electron microscopy (SEM) Analysis

Scanning Electron microscopy (SEM) was employed to characterize the surface morphology, particle size, and porosity of the synthesized materials. The activated carbon (AC) derived from plastic waste exhibited a relatively homogeneous surface with well-developed and abundant porous channels, which are favorable for pollutant adsorption through interactions with surface functional groups. The average particle size, determined using Image-J software (version 1.46r), was 63.29nm, in good agreement with crystallite size estimated from X-ray diffraction (XRD) analysis.

The zinc oxide (ZnO) sample displayed a heterogeneous surface morphology characterized by particles with variable sizes and shapes and the presence of multiple surface pores, features that are expected to enhance adsorption efficiency. The average particle size was 68.79nm confirming that the material falls within the nanoscale range. In the case of iron oxide ($Fe_2O_3$), SEM micrographs revealed an irregular surface morphology with numerous pores, and an average particle size of 91.69nm, further supporting the successful synthesis of nanoscale particles. The AC-$Fe_2O_3$/ZnO composite exhibited diverse porous channels and cavities with a relatively uniform surface texture. The average particle size of this composite was 72.11nm, confirming the effective loading of metal oxides onto the activated carbon and the formation of an efficient nanoscale adsorbent (Figure 3).

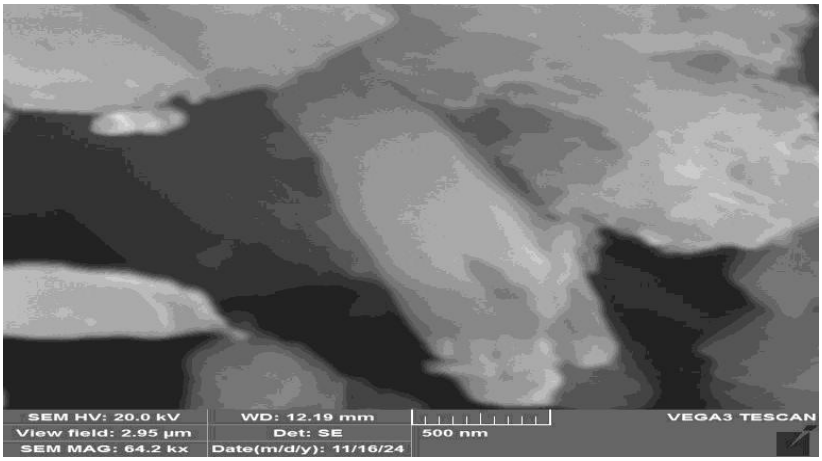


**Figure3.** The SEM morphology of AC-ZnO-$Fe_2O_3$ composite

### 3.5 Energy Dispersive X-ray (EDX) Analysis

Energy-dispersive X-ray spectroscopy (EDX) was used to determine the elemental composition of the prepared materials at room temperature, using an accelerating voltage in the range of 0-80 keV, based on the emission of characteristic X-rays from each element. The EDX spectrum of activated carbon (AC) derived from plastic waste showed the presence of carbon and oxygen, indicating successful surface oxidation and an increased oxygen content on the carbon matrix. For zinc oxide (ZnO), the EDX analysis confirmed the presence of zinc and oxygen, verifying the successful formation of ZnO nanoparticles. The $Fe_2O_3$ sample prepared via co-precipitation method exhibited iron and oxygen as the major elements, along with trace amounts of carbon, sodium, chlorine and silicon. These minor elements are attributed to residual precursors and impurities originating from the synthesis process.

In the AC-$Fe_2O_3$/ZnO composite, the carbon-to-oxygen ratio was approximately 1.08, indicating the successful loading and distribution of ZnO-$Fe_2O_3$ nanoparticles onto the activated carbon surface (Figure 4).

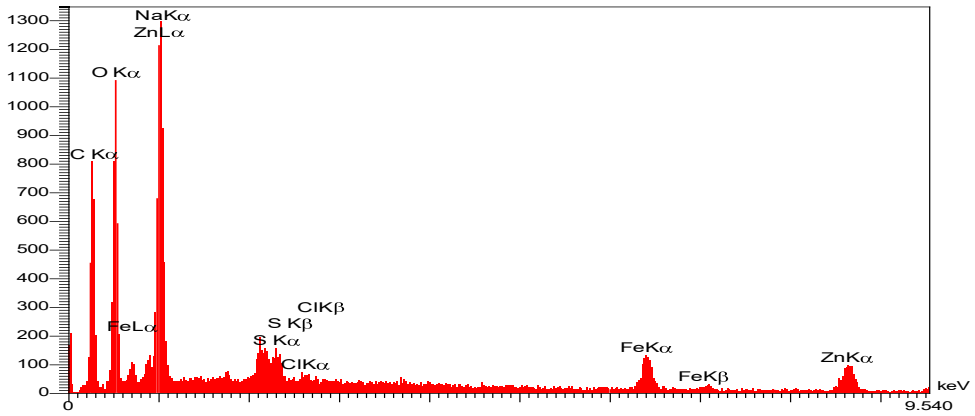


**Figure4.** The EDX result of AC-ZnO-$Fe_2O_3$ composite

### 3.6 Zeta potential measurement

Zeta potential measurement is an essential technique to determine the surface charge of material and evaluate their stability in aqueous solution. The zeta potential of the high stability with a value of -42.2mV, indicating a negative charged surface. The value of −42.2 mV signifies that the surface is strongly negative charged and stable. As Eosin Blue and Fuchsin Acid are anionic dyes, electrostatic repulsion may be generated between the dye molecules and the adsorbent surface. Therefore, the adsorption process is not mainly governed by electrostatic attraction, but mainly by the non-electrostatic interactions, including π–π stacking between the aromatic rings of the dyes and the graphitic structure of the activated carbon, hydrogen bonding between the functional groups of the dyes and the oxygen-containing groups (–OH and –COOH) on the surface, as well as the dispersion forces and surface interactions of the $Fe_2O_3$ and ZnO nanoparticles. Similar behavior has been reported for anionic dye adsorption onto negatively charged carbon-based composites [43] as shown in Figure 5.

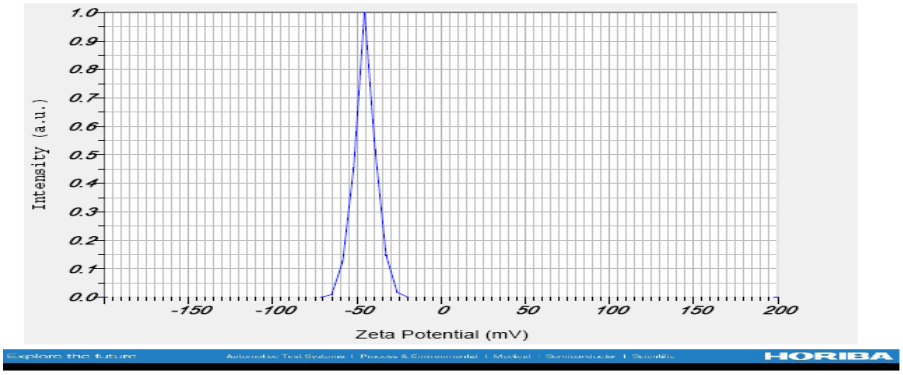


**Figure5.** The zeta potential result of AC-ZnO-$Fe_2O_3$ composite

### 3.7Adsorption

Four main parameters affecting the adsorption process were investigated namely: equilibrium contact time, solution pH, temperature, and agitation speed. Throughout these experiments, the adsorbent dosage (0.01g) and dye solution volume (10mL) were maintained constant. Eosin Blue and Fuchsin Acid were used as model pollutants at initial concentrations of 100mg/L and 200 mg/L, respectively.

#### 3.7.1 Effect of Equilibrium time

The effect of contact time on the adsorption of Eosin Blue and Fuchsin Acid onto AC-ZnO and $Fe_2O_3$ was investigated at intervals ranging 5, 10, 20 ,40 ,60 ,90 ,120 ,180 ,240 ,360 ,540 ,720 min. Experiment was performed at room temperature, natural pH, and agitation speed of 150 rpm, with initial concentrations of 100 mg/L for EB and 200 mg/L for (FA). Results showed

that removal efficiency increased with contact time, reaching equilibrium at 360 min (18.71%) for EB and 90 min (75.52%) for FA likely due to differences in dye structure and adsorbent surface charge (Figures 6-7).

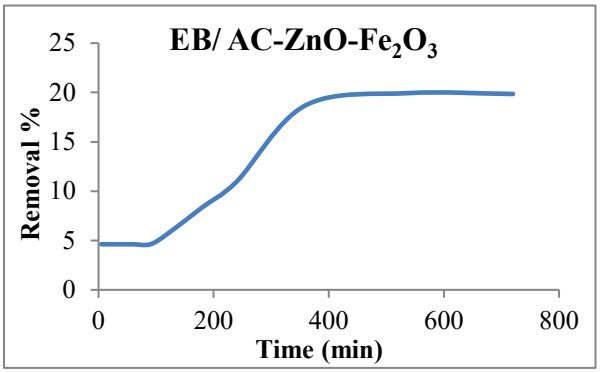


**Figure 7.** The effect of equilibrium time for FA

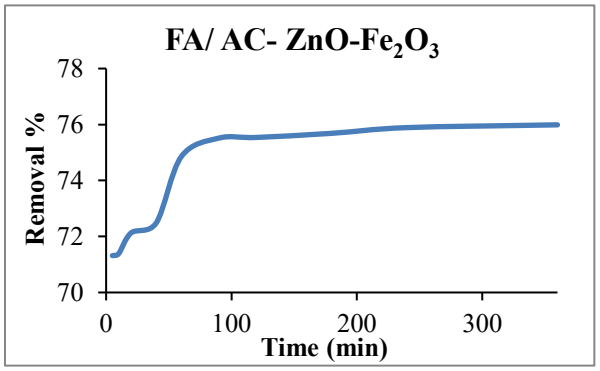


**Figure 6.** The effect of equilibrium time for **EB**

### 3.7.2 Effect of pH

The effect of pH on the adsorption of Eosin blue and Fuchsin Acid onto AC-ZnO-$Fe_2O_3$ was investigated by preparing dye solutions with fixed concentrations of 100 mg/L and 200 mg/L, respectively. Over a pH range of 3,4,5,6,7,8,9. experiment were conducted at room temperature, with agitation speed of 150rpm, using the previously determined equilibrium time for each dye.

The results revealed that the highest removal efficiency for Eosin blue was achieved at pH7 with 61.81%, followed by a gradual decrease at higher pH values, indicating electrostatic attraction between the different charged dye molecules and the adsorbent surface. In contrast, Fuchsin Acid exhibited a progressive increase in removal efficiency towards the alkaline range, reaching 87.73%, which can be attributed to the enhanced interaction between the different charge dye molecules and the adsorbent surface under basic condition (Figures 8-9).

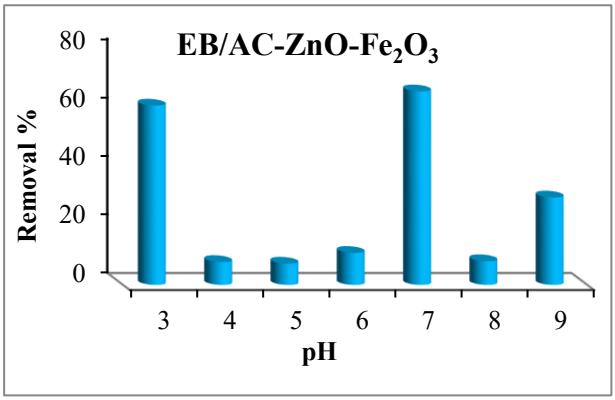


**Figure 8.** The effect of pH for EB

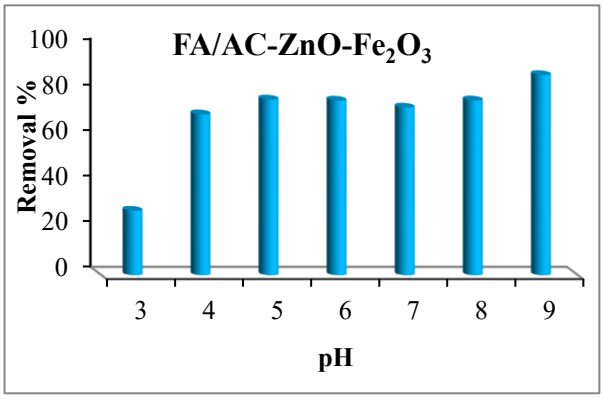


**Figure 9.** The effect of pH for FA

### 3.7.3 Effect of Temperature

The effect of temperature variation on the adsorption efficiency of Eosin blue and Fuchsin Acid onto from their aqueous solution onto AC-ZnO-$Fe_2O_3$ was investigated while keeping other parameters constant. Experiment was performed at different temperatures 25,35,45,55 and 65 $^{o}$C, to determine the optimal adsorption temperature for both dyes, using initial concentrations of 100 mg/L for EB and 200 mg/L for FA, an agitation speed of 150 rpm, and the predetermined equilibrium time and pH. A fixed solution volume (10 mL) and adsorbent dose (0.01g) were used in all experiments. The results showed that the adsorption efficiency of both dyes was highest at 25$^{o}$C, with removal percentage of 75.96% for EB and 88.10% for FA, as illustrated in Figures 10-11. The decrease in adsorption efficiency with increasing temperature indicates that the adsorption is overall exothermic, consistent with many dye–adsorbent systems where elevated temperature reduces interaction strength between dye molecules and surface-active sites.

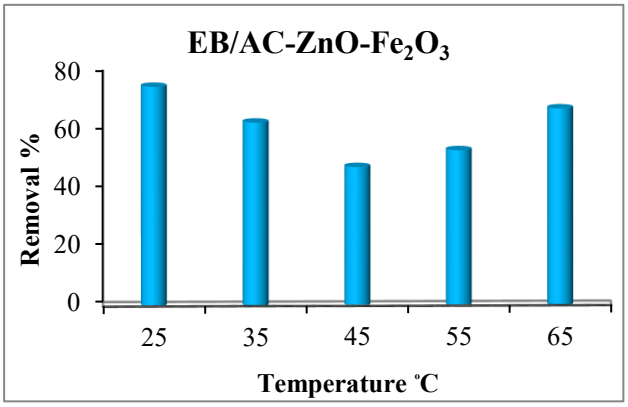


**Figure 10.** The effect of temperature for EB

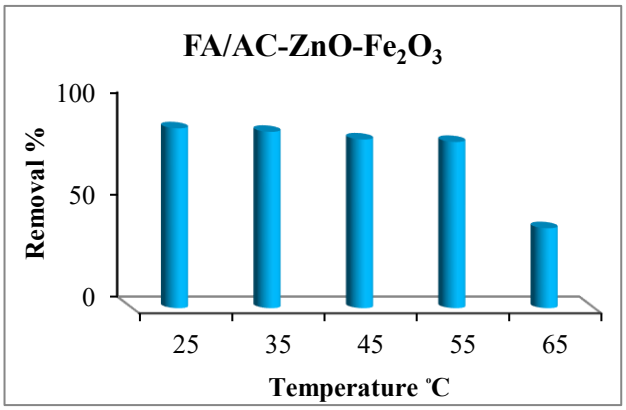


**Figure 11.** The effect of temperature for FA

### 3.7.4 Effect of agitation speed

The effect of agitation speed on the adsorption of Eosin blue and Fuchsin Acid from aqueous solution onto AC-ZnO-$FeO_3$ was studied while keeping the initial dye concentration constant at 100mg/L and 200 mg/L, respectively. A fixed dye solution volume (10mL) and adsorbent dose (0.01g) were used under the previously optimized conditions of pH, temperature, and contact time. The results showed that the highest adsorption efficiency was achieved at an agitation speed of 200 rpm, with removal percentage of 77.17% for Eosin blue and 88.21% for Fuchsin Acid, as illustrated in Figures12-13. The enhancement in adsorption with increasing stirring speed can be attributed to the improved diffusion rate of dye molecules toward the external surface of the adsorbent, reducing the boundary layer thickness and facilitating stronger interactions between the dye molecules and the active adsorption sites.

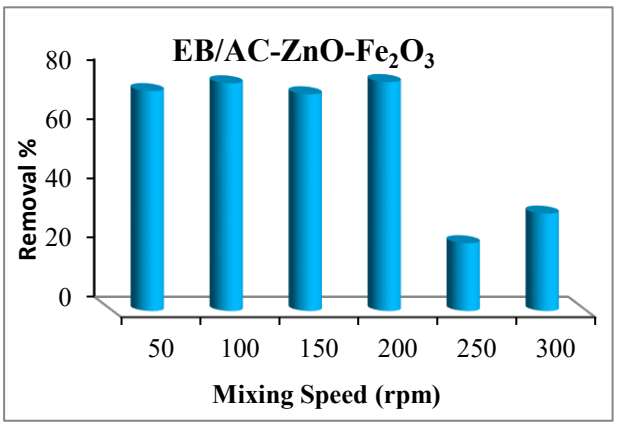


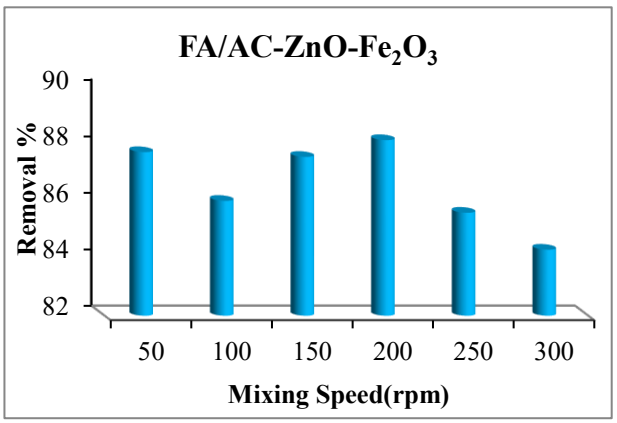


**Figure12.** The effect of agitation speed for EB **Figure13.** The effect of agitation speed for FA

After studying the four factors, the optimal conditions for the removal of Eosin blue and Fuchsin Acid were determined, as summarized in Table 2.

**Table 2.** The optimal condition for the adsorption process of Eosin Blue and Fuchsin Acid

| Dye name | $C_o$ mg/L | Temperature ºC | pH | Equilibrium time (min) | Agitation Speed rpm | Removal% |
|---|---|---|---|---|---|---|
| Eosin Blue (EB) | 100 | 25 | 7 | 360 | 200 | 77.17 |
| Fuchsin Acid (FA) | 200 | 25 | 9 | 90 | 200 | 88.21 |

### 3.7.5 Adsorption Isotherms

The adsorption isotherms were evaluated to understand the adsorption behavior, surface characteristics, and interaction mechanisms between Eosin Blue and Fuchsin Acid molecules and the AC-$Fe_2O_3$/ZnO composite. In addition, the isotherm analysis was used to assess the nature of the adsorption process and the type of binding interactions involved. The equilibrium data were analyzed using the Langmuir and Freundlich isotherm models. The calculated parameters, summarized in Table 3 and presented in Figures 14-15, indicate that the adsorption of both dyes onto the modified activated carbon is favorable. The Freundlich heterogeneity factor ($n > 1$) suggests favorable adsorption and reflects the heterogeneous surface interactions of the composite, with adsorption occurring on sites of different energies and affinities, consistent with a multilayer adsorption mechanism.

**Table3.** Freundlich constants for the adsorption of EB and FA

| Dyes | Temperature °C | N | $K_f$ | $R^2$ |
|---|---|---|---|---|
| Eosin Blue (EB) | 25 | 3.871828 | 31.34382 | 0.854 |
| | 35 | 3.189798 | 31.82782 | 0.890 |
| | 45 | 2.854542 | 31.19404 | 0.922 |
| | 55 | 2.85588 | 34.15859 | 0.900 |
| Fuchsin Acid (FA) | 25 | 2.107772 | 36.77251 | 0.954 |
| | 35 | 1.952858 | 32.19289 | 0.957 |
| | 45 | 1.82737 | 28.22733 | 0.958 |
| | 55 | 1.778619 | 27.04368 | 0.961 |

Furthermore, the correlation coefficients ($R^2$) show that the adsorption of Fuchsin Acid is better described by the Freundlich model, indicating adsorption on a heterogeneous surface. In contrast, Eosin Blue exhibits a relatively lower fit to the Freundlich model, suggesting slight differences in adsorption behavior and interaction mechanisms between the two dyes. The favorability of adsorption was further evaluated using the Langmuir separation factor ($R_L$), calculated as:

$$R_L = \frac{1}{1 + K_L\ C_0}$$

where:

$C_0$: is the initial dye concentration (mg/L)

$K_L$: is the Langmuir constant (L/mg)

$R_L$: is the dimensionless separation factor.

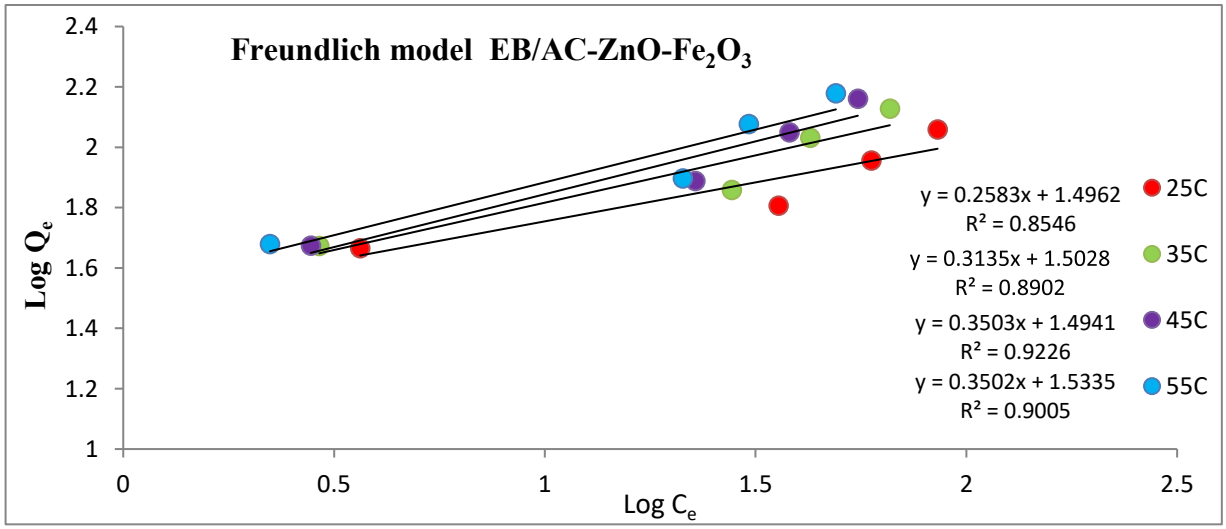


**Figure14**. Freundlich isotherm of Eosin Blue onto AC-ZnO-$Fe_2O_3$ composite

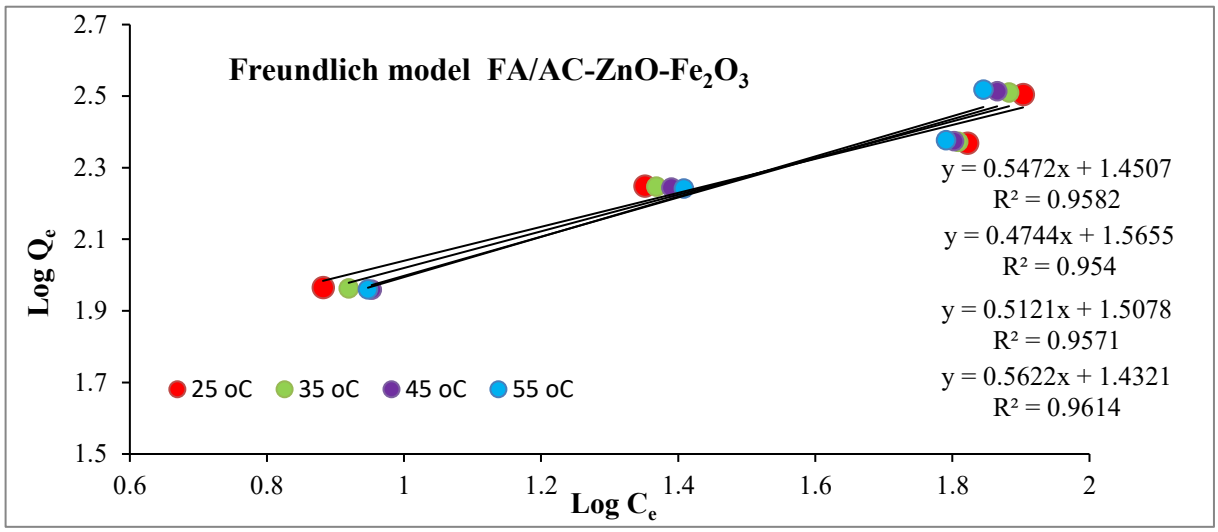


**Figure15.** Freundlich isotherm of Fuchsin Acid onto AC-ZnO-$Fe_2O_3$ composite

The adsorption results fitted to the Langmuir model indicate the formation of a monolayer adsorption system, which can be attributed to the homogeneity of the adsorbent surface and the chemical nature of the dyes. Figures 16-17 present the adsorption behavior of Eosin blue and Fuchsin Acid on AC-$Fe_2O_3$&ZnO, showing a closer fit of Fuchsin Acid to the Langmuir model compared to Eosin blue (Table 4). The maximum adsorption capacity ($Q_{max}$) was found to be 441.60 mg/g for Fuchsin Acid and 176.22 mg/g for Eosin Blue. Additionally, the separation factor ($R_L$) values lie within the range $0<R_L<1$, confirming that the adsorption system is favorable and that interactions between the dye molecules and the adsorbent occur efficiently on a homogeneous monolayer surface

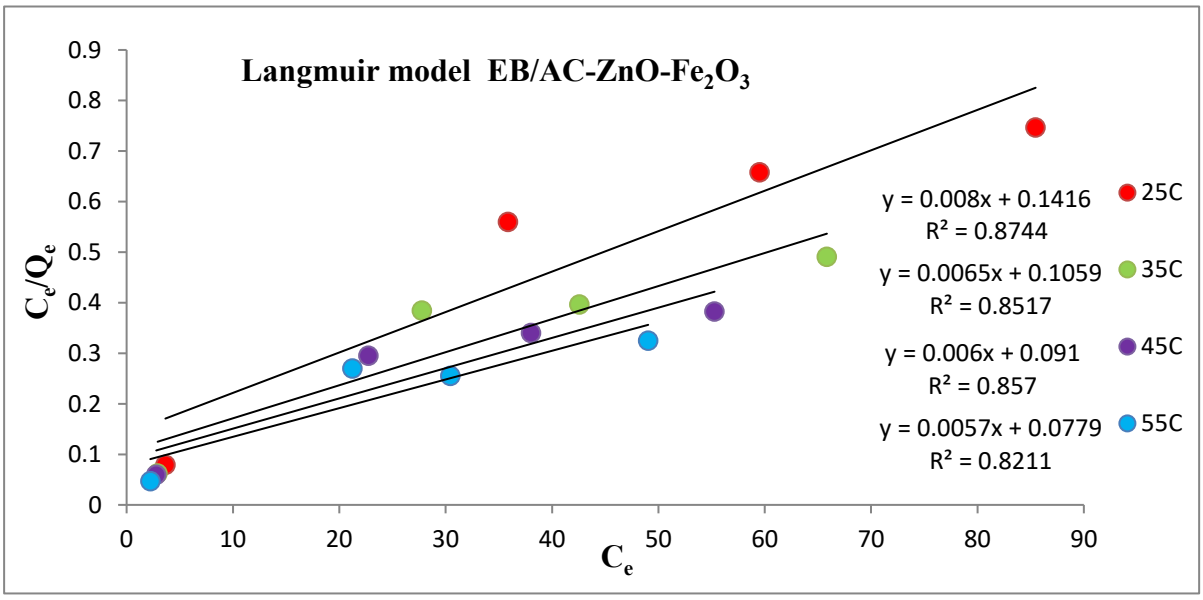


**Figure16.** Langmuir isotherm of Eosin Blue onto AC-ZnO-$Fe_2O_3$ composite

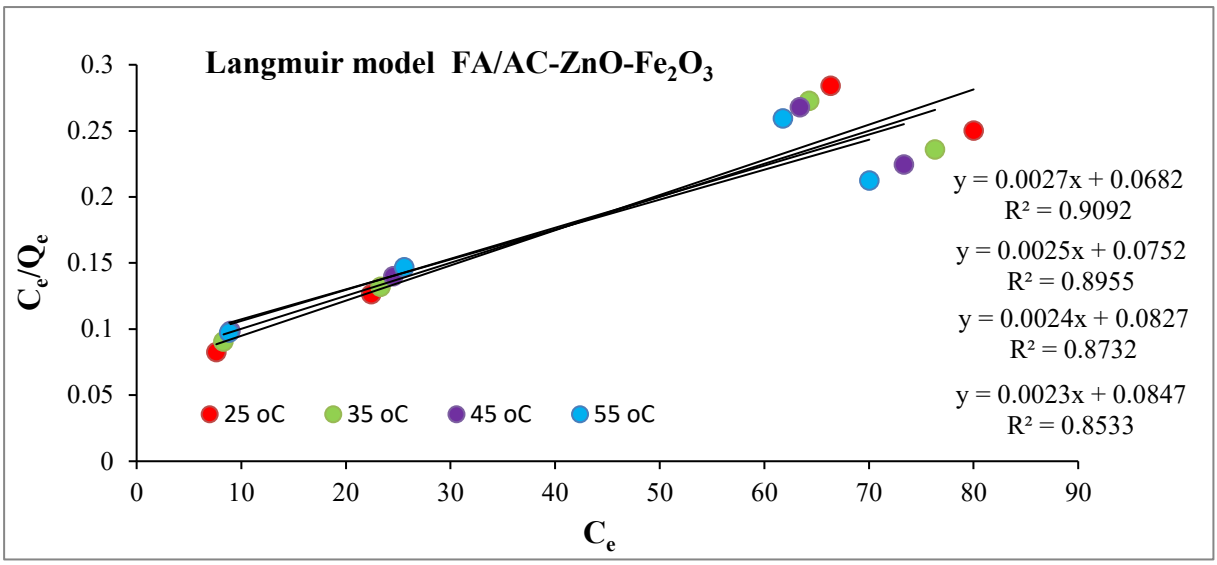


**Figure17.** Langmuir isotherm of Fuchsin Acid onto AC-ZnO-$Fe_2O_3$ composite

**Table 4.** Langmuir constants for the adsorption of EB and FA

| Dyes | Temperature °C | $Q_{max}$ (mg/g) | $K_L$ (L/mg) | $R_L$ | $R^2$ |
|---|---|---|---|---|---|
| Eosin Blue (EB) | 25 | 125.0258 | 0.056496 | 0.261452 | 0.982 |
| | 35 | 152.8847 | 0.061771 | 0.244585 | 0.988 |
| | 45 | 167.1524 | 0.065718 | 0.233323 | 0.968 |
| | 55 | 176.2279 | 0.072857 | 0.215386 | 0.613 |
| Fuchsin Acid (FA) | 25 | 375.4562 | 0.039032 | 0.203947 | 0.844 |
| | 35 | 400.3209 | 0.033216 | 0.231395 | 0.854 |
| | 45 | 425.4367 | 0.028436 | 0.260176 | 0.621 |
| | 55 | 441.6065 | 0.026725 | 0.272293 | 0.715 |

### 3.7.6 Thermodynamic study of the Adsorption process

Temperature plays a significant role in the adsorption process in solid-liquid systems and provides important information about the thermodynamic behavior of the system. Thermodynamic parameters such as Gibbs free energy ($\Delta G^o$), enthalpy($\Delta H^o$), and entropy ($\Delta S^o$) were evaluated to determine the spontaneity and nature of the adsorption [44]. The distribution coefficient (K), which represents the equilibrium between the amount of dye adsorbed on the solid and liquid phase and its concentration in the liquid phase, was calculated using:

$$K = \frac{Qe}{Ce}$$

The Gibbs free energy change was obtained from the relation:

$\Delta G^{O} = -RT \ln K$

Negative $\Delta G^{\circ}$ values indicate that adsorption is thermodynamically spontaneous under the studied conditions; however, spontaneity alone does not determine whether adsorption is purely physical or chemical. Mechanistic inference should be supported by the magnitude of thermodynamic parameters and complementary characterization. The relationship among thermodynamics functions follows the Gibbs equation [36]:

$\Delta G^{o} = \Delta H^{o} - T\Delta S^{o}$

The thermodynamic parameters ($\Delta H^{o}$, $\Delta S^{o}$, and $\Delta G^{o}$) were determined from the linear plots of ln K versus 1/T. The enthalpy change ($\Delta H^{o)}$ provides information about heat effect of the adsorption process, where a positive value indicates an endothermic process, while a negative value reflects exothermic behavior. The entropy change ($\Delta S^{o}$) represents the degree of randomness at the soild-solution interface; positive $\Delta S^{o}$ values suggest increased disorder and enhance affinity between the dye molecules and the adsorbent surface.

The calculated thermodynamic parameters for the adsorption of Eosin Blue (EB) and Fuchsin Acid (FA) onto the AC-$Fe_2O_3$/ZnO composite are presented in Tables 5-6 and illustrated in Figures 18-19. The negative $\Delta G^{o}$ values obtained for both dyes at all studied temperatures confirm the spontaneous adsorption process. The relatively low magnitude of $\Delta G^{o}$ further suggests that the adsorption is predominantly governed by physical interactions. For EB, positive values of $\Delta H^{o}$ and $\Delta S^{o}$ indicate that the adsorption process is endothermic and accompanied by an increase in randomness at the adsorbent-solution interface. In the case of FA, the negative $\Delta G^{o}$ values also confirm spontaneous adsorption, while the positive $\Delta S^{o}$ values reflect a strong affinity between the dye molecules and the composite surface. $\Delta H^{o}$ for FA exhibited concentration-dependent behavior, showing exothermic characteristics at low concentrations (100-200 mg/L) and endothermic behavior at higher concentrations. These results indicate that the adsorption of both dyes is spontaneous and primary physical in nature, with temperature playing a significant role in the influencing the adsorption mechanism and the strength of interaction.

**Table 5.** Thermodynamic faction result of EB

| $C_0$ | ΔH° | ΔS° | ΔG° kJ/mol | | | |
|---|---|---|---|---|---|---|
| mg/L | kJ/mol | J/mol/K | 298 °K | 308 °K | 318 °K | 328 °K |
| **50** | 13.1412 | 0.0653 | -6.2974 | -7.1222 | -7.4813 | -8.3578 |
| **100** | 20.0900 | 0.0727 | -1.4400 | -2.4493 | -3.2319 | -3.5752 |
| **150** | 16.5469 | 0.0886 | -10.039 | -10.451 | -11.730 | -12.588 |
| **200** | 13.4451 | 0.0795 | -9.9507 | -11.391 | -12.113 | -12.307 |

**Table 6.** Thermodynamic faction result of FA

| $C_0$ | ΔH° | ΔS° | ΔG° kJ/mol | | | |
|---|---|---|---|---|---|---|
| mg/L | kJ/mol | J/mol/K | 298 °K | 308 °K | 318 °K | 328 °K |
| **100** | -4.74964 | 0.004648 | -6.18328 | -6.15017 | -6.12725 | -6.35688 |
| **200** | -4.08991 | 0.003503 | -5.12415 | -5.18576 | -5.20123 | -5.23452 |
| **300** | 2.361965 | 0.018417 | -3.11935 | -3.32738 | -3.48213 | -3.68122 |
| **400** | 4.390698 | 0.026256 | -3.43449 | -3.6996 | -3.94925 | -4.227 |

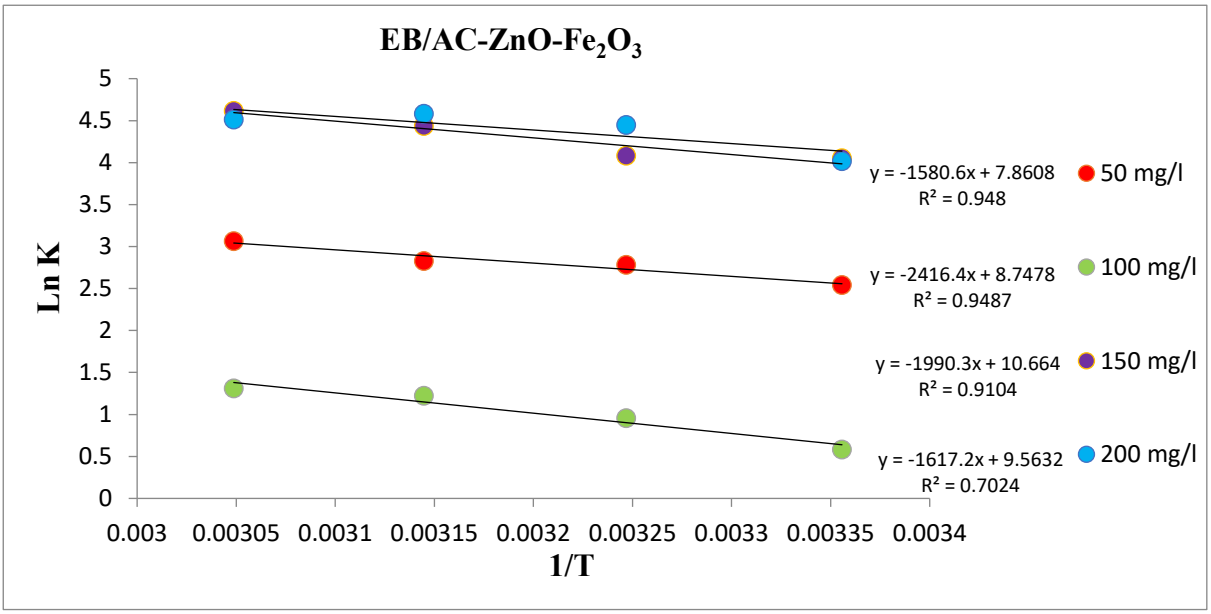


**Figure18.** Thermodynamic faction result of EB

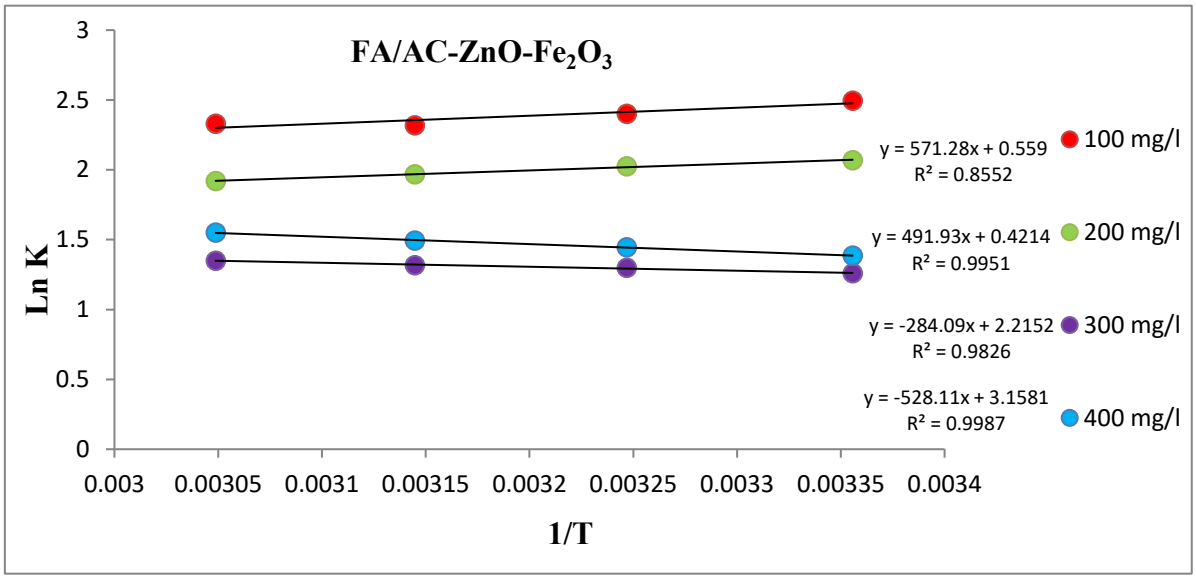


**Figure19.** Thermodynamic faction result of FA

### 3.7.7 Recovery study

The desorption behavior of Eosin Blue (100mg/L) and Fuchsin Acid (200mg/L) from AC-Fe2O3/ZnO composite was evaluated using distilled water as a polar desorbing agent under continuous agitation. The desorption process was carried out in two successive stages to assess the regeneration efficiency of the adsorbent. For Eosin Blue, desorption efficiencies of 70.99% and 27.4% were achieved in the first and second stages, respectively, resulting in a total recovery of 98.46%. In contrast, Fuchsin Acid exhibited a lower cumulative recovery of 75.81% after two desorption cycles, indicating stronger interactions between the dye molecules and the adsorbent surface. The reduced recovery efficiency observed for FA may be attributed to stronger surface interactions, possible diffusion limitations within the pore structure, and the influence of molecular size and polarity on the desorption process (Figure20).

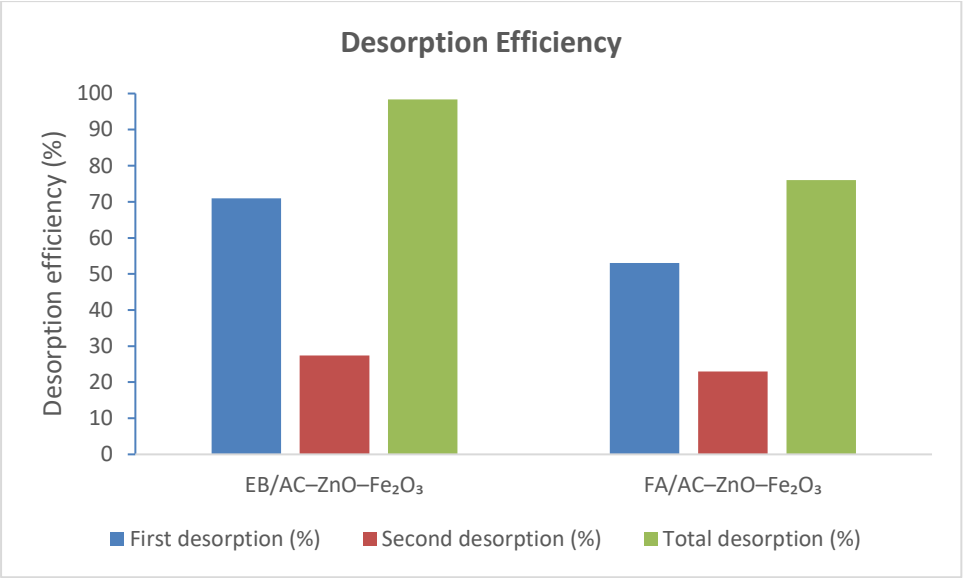


**Figure20.** Desorption efficiency of Eosin Blue and Fuchsin Acid from AC-ZnO-$Fe_2O_3$ composite

## 4. Conclusions

The AC-ZnO-$Fe_2O_3$ composite was successfully synthesized via a simple and environmentally sustainable approach using plastic waste derived activated carbon as a support for metal oxide nanoparticles. Comprehensive characterization and surface analyses (FTIR, EDX, XRD, BET, SEM and zeta potential) confirmed the successful formation of a stable composite with heterogeneous surface properties and enhance surface functionality. The material exhibited high adsorption performance toward the studied anionic dyes, with a maximum adsorption capacity of 441.60 mg/g for Fuchsin Acid and 176.22 mg/g for Eosin Blue, indicating strong affinity and effective interaction between the adsorbent and dye molecules. Isotherm analysis revealed heterogeneous multilayer adsorption behavior, while thermodynamic results indicated that the adsorption process for both dyes was spontaneous and predominantly endothermic, with the exception of Fuchsin Acid at concentrations of 100 and 200 mg/L, where the process became exothermic. The integration of waste valorization with enhanced adsorption performance highlights the material as a low-cost and sustainable candidate for efficient treatment of dye contaminated wastewater.

**References**

[1] R. P. K. Dasanayaka, "Applications of activated carbon in wastewater treatment as a low-cost media," *International Journal of Engineering Applied Sciences and Technology*, vol. 5, no. 7, pp. 210-217, 2020. https://doi.org/10.33564/IJEAST.2021.v05i11.001

[2] B. Alvez-Tovar, P. S. Scalize, G. Angiolillo-Rodríguez, A. Albuquerque, M. N. Ebang, and T. F. de Oliveira, "Agro-industrial waste upcycling into activated carbons: A sustainable approach for dye removal and wastewater treatment," *Sustainability*, vol. 17, no. 5, p. 2036, 2025. https://doi.org/10.3390/su17052036

[3] M. M. Rahman, "Waste biomass derived chitosan-natural clay-based bio nanocomposites fabrication and their potential application on wastewater purification by continuous adsorption: A critical review," *South African Journal of Chemical Engineering*, vol. 48, no. 1, pp. 214-236, 2024. https://doi.org/10.1016/j.sajce.2024.02.006

[4] G. T. Tee, X. Y. Gok, and W. F. Yong, "Adsorption of pollutants in wastewater via biosorbents, nanoparticles and magnetic biosorbents: A review," *Environmental Research*, vol. 212, no. Part B, p. 113248, 2022. https://doi.org/10.1016/j.envres.2022.113248

[5] B. Preetha and B. Vishalakshi, "Karaya gum-graft-poly (N, N' dimethylacrylamide) gel: A pH responsive potential adsorbent for sequestration of cationic dyes," *Journal of Environmental Chemical Engineering*, vol. 8, p. 103608, 2020. https://doi.org/10.1016/j.jece.2019.103608

[6] P. Xu, G. M. Zeng, D. L. Huang, C. L. Feng, S. Hu, M. H. Zhao, and Z. F. Liu, "Use of iron oxide nanomaterials in wastewater treatment: A review," *Science of The Total Environment*, vol. 424, pp. 1–10, 2012. https://doi.org/10.1016/j.scitotenv.2012.02.023

[7] Belgacem, I. Ould Brahim, M. Belmedani, and H. Hadoun, "Removal of methyl green dye from aqueous solutions using activated carbon derived from cryogenic crushed waste tires," *Iranian Journal of Chemistry and Chemical Engineering*, vol. 41, no. 1, pp. 207-219, 2022. https://doi.org/10.30492/IJCCE.2020.121562.3966

[8] R. Remmani, R. Makhloufi, M. Miladi, A. Ouakouak, A. R. Canales, and D. Núñez-Gómez, "Development of low-cost activated carbon towards an eco-efficient removal of organic pollutants from oily wastewater," *Polish Journal of Environmental Studies*, vol. 30, no. 2, pp. 1-8, 2021. https://doi.org/10.15244/pjoes/125765

[9] Kareem and A. J. Mohammed, "Removal of brilliant dyes from its aqueous solution by adsorption on siliceous rocks," *Systematic Reviews in Pharmacy*, vol. 11, no. 4, pp. 725–730, 2020.

[10] Nayeri and S. A. Mousavi, "Dye removal from water and wastewater by nanosized metal oxides - modified activated carbon: a review on recent researches," *Journal of Environmental Health Science and Engineering*, 2020. https://doi.org/10.1007/s40201-020-00566-w

[11] Elizondo-Villarreal, E. Gandara-Martínez, M. García-Méndez, M. Gracia-Pinilla, A. M. Guzmán-Hernández, V. M. Castaño, and C. Gómez-Rodríguez, "Synthesis and characterization of SiO2 nanoparticles for application as nanoadsorbent to clean wastewater," *Coatings*, vol. 14, no. 7, p. 919, 2024. https://doi.org/10.3390/coatings14070919

[12] Bosveli, T. Montagnon, Y. Kalaitzakis, and G. Vassilikogiannakis, "Eosin: a versatile organic dye whose synthetic uses keep expanding," *Organic & Biomolecular Chemistry*, vol. 19, no. 13, pp. 3303-3317, 2021. https://doi.org/10.1039/d0ob03013a

[13] H. Rahman, "Utilization of eosin dye as an ion pairing agent for determination of pharmaceuticals: A brief review," *International Journal of Pharmacy and Pharmaceutical Sciences*, vol. 9, no. 12, pp. 1-9, 2017. https://doi.org/10.22159/ijpps.2017v9i12.21220

[14] S. Krishnan, S. Chatterjee, A. Solanki, N. Guha, M. K. Singh, A. K. Gupta, and D. K. Rai, "Aminotetrazole-functionalized $SiO_2$ coated MgO nanoparticle composites for removal of acid fuchsin dye and detection of heavy metal ions," *ACS Applied Nano Materials*, vol. 3, no. 1, pp. 123-134, 2020. https://doi.org/10.1021/acsanm.0c02351

[15] El Haddad, "Removal of Basic Fuchsin dye from water using mussel shell biomass waste as an adsorbent: Equilibrium, kinetics, and thermodynamics," *Journal of Taibah University for Science*, vol. 10, no. 5, pp. 664-674, 2015. https://doi.org/10.1016/j.jtusci.2015.11.010

[16] F. Kordbacheh and G. Heidari, "Water pollutants and approaches for their removal," *Materials Chemistry Horizons*, vol. 2, no. 2, pp. 139–153, 2023.

[17] R. Foroutan, R. Mohammadi, and B. Ramavandi, "Elimination performance of methylene blue, methyl violet, and Nile blue from aqueous media using AC/CoFe2O4 as a recyclable magnetic composite," *Environmental Science and Pollution Research*, vol. 26, no. 17, pp. 17431-17443, 2019. https://doi.org/10.1007/s11356-019-05282-z

[18] R. Rashid, I. Shafiq, P. Akhter, M. J. Iqbal, and M. Hussain, "A state-of-the-art review on wastewater treatment techniques: the effectiveness of adsorption method," *Environmental Science and Pollution Research*, vol. 28, no. 8, pp. 9050-9066, 2021. https://doi.org/10.1007/s11356-021-12395-x

[19] M. I. Mohammed, A. A. Abdul Razak, and D. A. H. Al-Timimi, "Modified multiwalled carbon nanotubes for treatment of some organic dyes in wastewater," *Advances in Materials Science and Engineering*, vol. 2014, Article ID 201052, 2014. https://doi.org/10.1155/2014/201052

[20] Wang, J. Lan, C. Bo, B. Gong, and J. Ou, "Adsorption of heavy metal onto biomass-derived activated carbon: Review," *RSC Advances*, vol. 13, pp. 4275-4302, 2023. https://doi.org/10.1039/D2RA07911A

[21] Khan, K. Saeed, and I. Khan, "Nanoparticles: Properties, applications and toxicities," *Arabian Journal of Chemistry*, vol. 12, pp. 908-931, 2017. https://doi.org/10.1016/j.arabjc.2017.05.011

[22] M. Kumari, G. R. Chaudhary, S. Chaudhary, and A. Umar, "Transformation of solid plastic waste to activated carbon fibres for wastewater treatment," *Chemosphere*, vol. 294, p. 133692, 2022. https://doi.org/10.1016/j.chemosphere.2022.133692

[23] O. H. Aremu, C. O. Akintayo, E. B. Naidoo, S. M. Nelana, and O. S. Ayanda, "Synthesis and applications of nano-sized zinc oxide in wastewater treatment: a review," *International Journal of Environmental Science and Technology*, vol. 18, no. 10, pp. 3237–3256, 2021. https://doi.org/10.1007/s13762-020-03069-1

[24] P. Kumari, M. Alam, and W. A. Siddiqi, "Usage of nanoparticles as adsorbents for waste water treatment: An emerging trend," *Sustainable Materials and Technologies*, vol. 22, p. e00128, 2019. https://doi.org/10.1016/j.susmat.2019.e00128

[25] L. Dinesha, H. Sharanagouda, N. Udaykumar, C. T. Ramachandr, and A. B. Dandekar, "Removal of pollutants from water/waste water using nano-adsorbents: A potential pollution mitigation," *International Journal of Current Microbiology and Applied Sciences*, vol. 6, no. 10, pp. 4868-4872, 2017. https://doi.org/10.20546/ijcmas.2017.610.455

[26] Y. Ristianingsih, P. Perwitasari, I. Lestari, T. T. Anastasia, and A. Amrullah, "Enhanced methylene blue adsorption using $Fe_2O_3$-modified brown algae activated carbon," *Reaction Kinetics, Mechanisms and Catalysis*, pp. 4153-4170, 2025.

[27] S. Ayyalusamy and S. Mishra, "Optimization of preparation conditions for activated carbons from polyethylene terephthalate using response surface methodology," *Brazilian Journal of Chemical Engineering*, vol. 35, no. 3, pp. 1105-1116, 2018. https://doi.org/10.1590/0104-6632.20180353s20160724

[28] N. D. Kandpal, N. Sah, R. Loshali, R. Joshi, and J. Prasad, "Co-precipitation method of synthesis and characterization of iron oxide nanoparticles," *Journal of Scientific & Industrial Research*, vol. 73, pp. 87-90, 2014.

[29] Z. L. S. Seow, A. S. W. Wong, V. Thavasi, R. Jose, S. Ramakrishna, and G. W. Ho, "Controlled synthesis and application of ZnO nanoparticles, nanorods and nanospheres in dye-sensitized solar cells," *Nanotechnology*, vol. 20, no. 4, p. 045604, 2008. https://doi.org/10.1088/0957-4484/20/4/045604

[30] M. A. Raheem, Z. A. Abdulnabi, and A. A. Al-Shawi, "Synthesis and characterization of multiwalled carbon nanotubes decorated by ZnO and Ag2O for using to remove methyl green and erythrosin B dyes from their aqueous solutions," *Advances in Chemical Science and Engineering*, vol. 49, no. 1, pp. 1-11, 2025. https://doi.org/10.18280/acsm.490111

[31] M. Afroze and T. K. Sen, "A review on heavy metal ions and dye adsorption from water by agricultural solid waste adsorbents," *Water Air & Soil Pollution*, vol. 229, p. 225, 2018. https://doi.org/10.1007/s11270-018-3910-3

[32] R. Foroutan, H. Esmaeili, S. D. Rishehri, F. Sadeghzadeh, S. Mirahmadi, M. Kosarifard, and B. Ramavandi, "Zinc, nickel, and cobalt ions removal from aqueous solution and plating plant wastewater by modified Aspergillus flavus biomass: A dataset," *Data in Brief*, vol. 12, pp. 485-492, 2017. https://doi.org/10.1016/j.dib.2017.04.031

[33] N. Bahramifar, M. Tavasoli, and H. Younesi, "Removal of eosin Y and Eosin blue dyes from polluted water through biosorption using Saccharomyces cerevisiae: Isotherm, kinetic and thermodynamic studies," *Journal of Applied Research in Water and Wastewater*, vol. 2, no. 1, pp. 108-114, 2015.

[34] R. Kumar and J. Chawla, "Removal of cadmium ion from water/wastewater by nano-metal oxides: A review," *Water Quality, Exposure and Health*, 2013. https://doi.org/10.1007/s12403-013-0100-8

[35] J. Bayuo, M. J. Rwiza, J. W. Choi, K. Mtei, A. Hosseini-Bandegharaei, M. Sillanpää, G. Limousin, J. P. Gaudet, L. Charlet, S. Szenknect, V. Barthès, and M. Krimissa, "Adsorption and desorption processes of toxic heavy metals, regeneration and reusability of spent adsorbents: Economic and environmental sustainability approach," *Advances in Colloid and Interface Science*, vol. 329, p. 103196, 2024. https://doi.org/10.1016/j.cis.2024.103196

[36] Liu, Y. Liu, J. Peng, Z. Liu, Y. Jiang, M. Meng, W. Zhang, and L. Ni, "Preparation of high surface area oxidized activated carbon from peanut shell and application for the removal of organic pollutants and heavy metal ions," *Water, Air, & Soil Pollution*, vol. 229, p. 391, 2018. https://doi.org/10.1007/s11270-018-4021-9

[37] P. Punia, M. K. Bharti, S. Chalia, R. Dhar, B. Ravelo, P. Thakur, and A. Thakur, "Recent advances in synthesis, characterization, and applications of nanoparticles for contaminated water treatment- A review," *Ceramics International*, 2020. https://doi.org/10.1016/j.ceramint.2020.09.050

[38] T.-D. Hoang, Y. Liu, and M. T. Le, "Synthesis and Characterization of Biochars and Activated Carbons Derived from Various Biomasses," *Sustainability*, vol. 16, no. 13, p. 5495, 2024. https://doi.org/10.3390/su16135495

[39] M. I. Moustafa, M. M. El-Sayed, and H. S. Mahfouz, "Superparamagnetic Nano α-Fe2O3 and TiO2 as Photocatalysts and Adsorbents in Wastewater Treatment; Evaluation of Photocatalytic Activity and Biological Response," *International Journal of Nanotechnology in Medicine & Engineering*, vol. 6, no. 1, pp. 1-9, 2021.

[40] V. S. Vinila and J. Isac, "Synthesis and structural studies of superconducting perovskite GdBa2Ca3Cu4O10.5+ δ nanosystems," in *Design, Fabrication, and Characterization of Multifunctional Nanomaterials*, pp. 319-341, 2022. https://doi.org/10.1016/B978-0-12-820558-7.00022-4

[41] R. A. Jasim and R. H. Salman, "Use of nano Co–Ni–Mn composite and aluminum for removal of artificial anionic dye Congo red by combined system," *Ecological*

*Engineering & Environmental Technology*, vol. 25, no. 7, pp. 133–149, 2024. https://doi.org/10.12912/27197050/188266

[42] M. Ahmad, A. R. Abdul Aziz, S. A. Mazari, A. G. Baloch, and S. Nizamuddin, "Photocatalytic degradation of methyl orange from wastewater using a newly developed Fe–Cu–Zn–ZSM-5 catalyst," *Environmental Science and Pollution Research*, vol. 27, pp. 21349–21363, 2020. https://doi.org/10.1007/s11356-020-08940-9

[43] L. Fernández-Peña, E. Guzmán, F. Ortega, L. Bureau, F. Leaoforte, D. Velasco, R. Rubio, and G. Luengo, "Physico-chemical study of polymer mixtures formed by a polycation and a zwitterionic copolymer in aqueous solution and upon adsorption onto negatively charged surfaces," *Polymer*, 2024. https://doi.org/10.1016/j.polymer.20

[44] P. Karthikeyan and S. Meenakshi, "Removal of toxic ions from aqueous solutions by surfactant-assisted biopolymeric hybrid membrane: Synthesis, characterization and toxic ions removal performance," *Journal of Environmental Chemical Engineering*, vol. 8, no. 3, p. 103717, 2020. https://doi.org/10.1016/j.jece.2020.103717

## الامتزاز عالي الكفاءة والامتزاز المستدام للأصباغ الانيونية بأستخدام متراكب جديد من AC-ZnO-$Fe_2O_3$

**آيات صلاح مهلهل[1] ودنيا علي حسين[1] وزهير علي عبدالنبي[2]**

[1] قسم البيئة، كلية العلوم، جامعة البصرة، البصرة، العراق.

[2] قسم الكيمياء البحرية، مركز علوم البحار، جامعة البصرة، البصرة، العراق.

**المستخلص**

هدفت هذه الدراسة إلى تحضير وتوصيف مادة نانوية مركبة جديد ماصة عالية الكفاءة مكون من الكربون المنشط المحمل بأكاسيد الزنك والحديد (AC-ZnO-$Fe_2O_3$) مطورة من الكربون المنشط المستخلص من النفايات البلاستيكية وجسيمات أكاسيد المعادن النانوية، وذلك لإزالة صبغة الايوسين الأزرق وحامض الفوشين من المحاليل المائية بشكل مستدام. تم توصيف الخصائص الفيزيائية والكيميائية والبنيوية والمورفولوجية للمادة المحضرة باستخدام تقنيات FTIR و XRDو FE-SEM و EDX و BET وتحليل جهد زيتا. وأكدت نتائج تجارب الامتزاز تحقق اعلى كفاءة ازالة بلغت 77.17% و 88.21% لكل من صبغتي الايوسين الازرق وحامض الفوشين على التوالي. وكشفت دراسات الاتزان ان بيانات الامتزاز تتوافق بشكل أفضل مع نموذج فريندلش مما يشير إلى حدوث امتزاز متعدد الطبقات على سطح غير متجانس. واشار التحليل الديناميكي الحراري إلى الطبيعة التلقائية لعملية الامتزاز (GΔ° سالبة)، التي كانت ماصة للحرارة في الغالب. كما اظهرت تجارب الاسترجاع امكانية اعادة استخدام المادة بكفاءة عالية، إذ بلغت نسب الاسترجاع 98.46% لصبغة الإيوسين الأزرق و75.81% لصبغة حامض الفوشين باستخدام الماء كمذيب. ويستنتج أن المركب النانوي المحضر يعد مادة ماصة فعالة ومنخفضة التكلفة ومستدامة بيئيًا لمعالجة المياه العادمة الصناعية الملوثة بالأصباغ وإعادة استخدامها.

**الكلمات المفتاحية:** الكاربون المنشط، الايوسين الازرق، الفوشين، اوكسيد الزنك، الملوثات العضوية، الاسترجاع.